Plate tectonics on the early Earth: limitations imposed by strength and buoyancy of subducted lithosphere

Jeroen van Hunen
Arie P. van den Berg

August 16, 2006

Abstract

The tectonic style and viability of modern plate tectonics in the early Earth is still debated. Field observations and theoretical arguments both in favor and against the uniformitarian view of plate tectonics back until the Archean continue to accumulate. Here, we present the first numerical modeling results that address for a hotter Earth the viability of subduction, one of the main requirements for plate tectonics. A hotter mantle has mainly two effects: 1) viscosity is lower, and 2) more melt is produced, which in a plate tectonic setting will lead to a thicker oceanic crust and harzburgite layer. Although compositional buoyancy resulting from these thick crust and harzburgite might be a serious limitation for subduction initiation, our modeling results show that eclogitization significantly relaxes this limitation for a developed, ongoing subduction process. Furthermore, the lower viscosity leads to more frequent slab breakoff, and sometimes to crustal separation from the mantle lithosphere. Unlike earlier propositions, not compositional buoyancy considerations, but this lithospheric weakness could be the principle limitation to the viability of plate tectonics in a hotter Earth. These results suggest a new explanation for the absence of ultrahigh-pressure metamorphism (UHPM) and blueschists in most of the Precambrian: early slabs were not too buoyant, but too weak to provide a mechanism for UHPM and exhumation.

1 Introduction

The viability of the plate tectonic process in a hotter, young Earth has been the subject of debate for decades (Vlaar, 1985, 1986; Vlaar and van den Berg, 1991; Davies, 1992; de Wit, 1998; Hamilton, 1998; van Thienen et al., 2004c; Stern, 2005). The arguments used sofar are mainly based on interpretation of geological observables and on simplified, parameterized modeling experiments. It is commonly assumed that the Earth has been cooling since the Archean and Proterozoic, but the amount of cooling is still uncertain. High-MgO Archean komatiites, for example, suggest a mantle temperature up to 350 K higher than today, whereas high grade terrains suggest that continental geotherms remained almost unchanged since the Archean (England and Bickle, 1984; Vlaar, 1986; Herzberg, 1992; de Wit, 1998). The importance of this debate lies in the geodynamical consequences: a different mantle temperature may have a large impact on the type of the dominant tectonic regime and the vigor of the associated circulation. Different theoretical models offer a wide spectrum of possible thermal histories for the Earth: On the one hand, in a hot mantle, the mantle viscosity drops considerably, which may result in an increasing vigor of convection. Most parameterized convection models based on heatflow (Q) - Rayleigh number (Ra) relationships $Q = CRa^{\beta}$ predict a 'thermal catastrophe': a hotter mantle is weaker and moves faster, leading to more surface heatflow and faster cooling. This faster cooling requires a hotter mantle starting temperature, which resulted in an even weaker mantle, etc. (e.g. Schubert et al., 2001). Recently, reduced values of C or β have been proposed to keep cooling within reasonable bounds throughout the Earth's history (e.g. Conrad and Hager, 2001; Grigné et al., 2005; Korenaga, 2005). On the other hand, more pressure-release partial melting occurs, producing thicker low-density layers of basaltic oceanic crust and underlying harzburgitic residual (Vlaar and van den Berg, 1991; van Thienen et al., 2004c), which increases the total lithospheric buoyancy. Today's plate tectonic mechanism is based on the gravitational instability of the subducting plates. If these plates remain buoyant, they cannot drive subduction. This idea has raised questions concerning the efficiency of plate tectonics to cool the early Earth (Vlaar, 1985, 1986; Vlaar and van den Berg, 1991; Davies, 1992; van Thienen et al., 2004c). Only very old plates would eventually become instable enough to drive the subduction process, but these old plates cannot cool the Earth sufficiently, especially with the higher level of radioactive heating in the past (Turcotte and Schubert, 2002; Sleep, 2000). These theoretical considerations indicate that the Earth's tectonics and convection could have been faster or slower in the past.

Within the plate-tectonic framework, several solutions to the latter problem are proposed. As an analogy to present day flat subduction of buoyant oceanic plateaus, shallow subduction of the buoyant lithosphere below overriding plates is suggested as the dominant style of subduction during the Proterozoic (Vlaar, 1986; Abbott et al., 1994). But van Hunen et al. (2004) showed that such style of subduction cannot have been effective in the early Earth due to the absence of gravitationally instable oceanic lithosphere with a thin crust, which today forms one of the main driving forces for the (shallow flat) subduction of oceanic plateaus. The basalt-to-eclogite transition will remove the compositional buoyancy (e.g. Peacock, 1993) and this applies equally well to the situation of a a thicker crust in a hotter Earth. The equilibrium depth of this transition is at around 40 km, although the reaction is known to be kinetically slow (Hacker, 1996; Austrheim, 1998). The density change during eclogitization is several times larger than any thermal density variations within the slab, and may have a profound influence on the subduction dynamics. The net effect of thermal and compositional buoyancy, and (kinetically retarded) crustal metamorphism in a hotter Earth with a thicker crust is not trivial, and we will elaborate on this influence in this study.

Alternatives for plate tectonics in the Archean have been proposed as well. A weak lowermost Archean crust may have resulted in a sandwich-like lithospheric rheology, in which 'flake tectonics' (Hoffman and Ranalli, 1988) or lower crust delamination (Vlaar et al., 1994; Parmentier and Hess, 1992; Zegers and van Keken, 2001) could have been active. Recently, van Thienen et al. (2004b) discussed related models of small-scale convection, large-scale resurfacing and hot diapir intrusion as possible Precambrian tectonic mechanisms.

Interpretation of geological observations has not reached consensus about the tectonic regime in the Precambrian. On the one hand, various sorts of evidence for Archean plate tectonics and subduction settings are proposed (e.g. de Wit, 1998; Komiya et al., 1999; Kusky et al., 2001), On the other hand, ultra-high pressure metamorphism (UHPM), which is commonly believed to be produced in subduction zones, does mostly occur later than about 600 Ma (personal communication H. L. M. van Roermund). This could be an indication for absence (Stern, 2005) or a changed style of plate tectonics. According to Hamilton (1998) voluminous magmatism, and not plate tectonics, dominated Archean secular cooling.

Most arguments that favor either absence or presence of plate tectonics in a hotter Earth were based on geological observations, theoretical considerations, or simple parameterized models. Here we present new results of a more complete numerical modeling study into the existence, vigor, and style of the plate tectonic process under hotter, early Earth circumstances. Operation of the subduction process is a minimum requirement for the existence of plate tectonics, and we have focused here on this key process, and consider a mantle convection model, were the mantle temperature is used as a discriminating control parameter in the experiments. First, the description of the governing equations, implemented compositional and phase transitions, rheological model, and the modeling setup and procedure are discussed. Then, we show the basic differences in subduction dynamics to be expected from a hotter mantle, and present sensitivity to the most important physical parameters. Finally, we discuss broader implications of these numerical model results, and relations to field observations such as the occurrence of ultrahigh-pressure metamorphism.

2 Model setup

A two-dimensional finite element model Sepran (Segal and Praagman, 2005) is used, which is based on the conservation of mass, momentum, energy, and composition, respectively:

$$\partial_j u_j = 0 \tag{1}$$

$$\partial_j(\eta\dot{\epsilon}_{ij}) - \partial_i \Delta P = \Delta\rho g_i \tag{2}$$

$$\rho c_p \left(\frac{\partial T}{\partial t} + u_j \partial_j T\right) - \alpha T \frac{dP}{dT} - \sum_k \rho_0 T \Delta S \frac{d\Gamma_k}{dt} - \partial_j(k\partial_j T) = \tau_{ij}\partial_j u_i + \rho_0 H \tag{3}$$

$$\frac{\partial C}{\partial t} + u_j \partial_j C = 0 \tag{4}$$

Symbols are explained in Table 1. Equation 1 states that the (incompressible) flow field is divergence-free, so that mass is conserved. The Stokes equation (Equation 2) implies that viscous and gravitational stresses are in equilibrium with the local dynamic pressure gradient (stresses due to inertia can be neglected in a slow-moving mantle). The (time-dependent) heat equation (Equation 3) describes the temperature change $\frac{\partial T}{\partial t}$ as a result of heat advection, adiabatic heating, latent heat effects from the mantle phase transitions, heat diffusion, viscous heating, and radiogenic heat production, respectively (van Hunen et al., 2001). Finally Equation 4 (also time-dependent) states that local changes of composition $\frac{\partial C}{\partial t}$ are due solely to advection of this field, i.e. composition is a non-diffusive quantity. Equations 1 and 2 fully describe the flow of mantle and lithosphere, but explicit solution of temperature T and composition C are necessary, because viscosity η (described below) and density variation $\Delta\rho$ are T- and C-dependent:

$$\Delta\rho(T, C, \Gamma_k) = \rho_0 \left[\sum_k \frac{\delta\rho_k}{\rho_0}\Gamma_k + \frac{\Delta\rho_c}{\rho_0} - \alpha(T - T_s)\right] \tag{5}$$

Equations 3 and 4 are, in turn, linked to the flow field through the non-linear coupling term describing advective transport.

The model domain is a closed 2000 km deep and 3600 km wide rectangular box with free-slip boundary conditions, and a thermally steady state continental lithosphere with a 70 mW/m^3 surface heat flow (maintained through local internal heating) adjacent to a 2500-km long oceanic lithosphere (Figure 1). Given the short timespan of the model calculations (see below), the box size and surface heat flow have very little influence on the dynamics of the flow as a result of secular temperature variations. Below the lithosphere, the initial thermal condition is an adiabatic temperature profile with given potential temperature T_{pot}. A 100 km deep subduction fault at an (arbitrarily chosen) fixed 2700 km distance from the mid-ocean ridge decouples the shallowest parts of the oceanic and continental lithospheres. This fault has a spline shape to ensure enough 'smoothness', and its angle with the horizontal increases to 45^o at its deepest point. Based on comparison of numerical experiments with geoid and topography observations (Zhong and Gurnis, 1992, 1994), and earthquake studies (Kanamori, 1980), the shear stress on major tectonic faults is expected to be low (lower than 30 MPa), and by default we impose the subduction fault to be free-slip. However, we also show results of subduction calculations with non-zero fault friction f_f.

2.1 Compositional and phase transitions

The potential temperature T_{pot} of the mantle (i.e. the adiabatic extrapolation of the mantle temperature to the surface) is varied between $\Delta T_{pot} = 0$K (i.e. $T_{pot} = 1350^o$C, the present-day situation) and $\Delta T_{pot} = 300$K for a younger Earth in steps of 100 K. For the present day situation (a 7 km thick oceanic crust), we assume a 36 km thick harzburgitic layer, of which the density difference with the underlying undepleted lherzolite $\delta\rho$ tapers linearly from -75 kg/m^3 at the top, to 0 kg/m^3 at its bottom. For $\Delta T_{pot} = 100$, 200, and 300K, a crustal thickness of 10, 15 and 22 km are taken, respectively (Figure 3, van Thienen et al., 2004c), and a constant ratio of crustal to harzburgitic layer thickness is assumed.

The major mantle phase transitions at 400 and 670 km depth are implemented under equilibrium conditions (i.e. no kinetic delay) (Christensen and Yuen, 1985), including the latent heat effects (van Hunen et al., 2001). Density differences across these transitions, and Clapeyron slopes from Bina and Helffrich (1994) are shown in Table 1. The 400-km discontinuity applies to both crust and mantle material, but the 670 km only applies to mantle material, as crustal material transforms to a denser phase deeper (Irifune and Ringwood, 1993).

When basalt (with $\rho = 2800\,\mathrm{kg/m^3}$ or $\delta\rho = -500\,\mathrm{kg/m^3}$ with respect to fertile mantle material (Peacock, 1993; Hacker, 1996)) transforms into eclogite (with $\delta\rho = +100\,\mathrm{kg/m^3}$), the compositional buoyancy of the crust and harzburgite changes sign. Basaltic metastability in the eclogite stability field directly influences the lithospheric buoyancy, and is therefore an important, but unfortunately rather poorly constrained phenomenon: temperature is widely believed to play a key role, but complete transformation at 250^oC and incomplete transformation at 800^oC have both been observed (Hacker, 1996). Also water content is likely to play an important role (Ahrens and Schubert, 1975; Rubie, 1990). Here, we model these kinetics with a simple parameterization: we assume a kinetic transition occurring in 1 or 5 Ma after entering the eclogite stability field (i.e. at pressures larger than 1.2 GPa). We ignored the fairly low topography of this transition as a result of temperature variations because of the small Clapeyron slope of about 1 MPa/K (Philpotts, 1990).

2.2 Rheological model

A warmer-than-today mantle is also weaker due to the temperature dependence in the rheological flow laws. This affects the coupling between mantle and plates, the ability of the plates to descend into the mantle, and the strength of the slabs (van Hunen et al., 2000). The material strength is described by a composite rheology of temperature and pressure dependent diffusion and dislocation creep (van den Berg et al., 1993; Karato and Wu, 1993) for crust and mantle material separately, a Byerlee pseudo-brittle deformation strength τ_{By}, and a uniform stress limiter τ_y. The total, effective viscosity is described as a combination of individual effective viscosities η_m of each mechanism m:

$$\eta_{\text{eff}} = \left(\sum_m (\eta_m)^{-1} \right)^{-1} \tag{6}$$

For two deformation mechanisms, diffusion creep and dislocation creep, an Arrhenius flow law is used:

$$\eta_m = A_m^{-1/n_m} \dot{\epsilon}^{(1-n_m)/n_m} \exp\left(\frac{E_m^* + pV_m^*}{n_m RT} \right) \tag{7}$$

with $\dot{\epsilon}$ the second invariant of the strainrate tensor. Default parameter values are taken from literature on laboratory studies: values in (Karato and Wu, 1993, dry rheology) are used for mantle material, and diabase values reported in (Shelton and Tullis, 1981) are taken for oceanic crust. Diffusion creep is not considered for crustal material. These and other creep parameters are summarized in Table 2.

Byerlee's 'law' (Kohlstedt et al., 1995) is approximated as $\tau_{By} = \tau_0 + \mu\rho_0 gz$, with $\tau_0 = 10$ MPa, and $\mu = 0.2$. The effective 'Byerlee viscosity' is then given by $\eta_{By} = \frac{\tau_{By}}{\dot{\epsilon}}$ (see Table 1).

The material-independent stress limiting rheology is described in terms of a powerlaw yield viscosity

$$\eta_y = \tau_y \dot{\epsilon}_y^{\frac{1}{n_y}} \dot{\epsilon}^{\frac{1}{n_y}-1} \tag{8}$$

to limit the strength of the material to approximately the yield stress τ_y without unrealistically 'brittle' properties at large depth. In this study, $\dot{\epsilon}_y = 10^{-15}$ s^{-1} and $n_y = 10$ were chosen. τ_y is a rather poorly known parameter, and several values between between 100 MPa and 1 GPa are examined. This stress limiter effectively replaces other deformation mechanisms, such as the Peierl's mechanism (Kameyama et al., 1999), which are not implemented here.

Previous studies have shown that hydration of the mantle wedge probably makes this region at least an order of magnitude weaker than elsewhere under similar, but drier conditions (Billen and Gurnis, 2001; Kukačka and Matyska, 2004). In models with slab pull as the main driving force for subduction, such as presented in this study, a strong mantle wedge without hydration results in a strong coupling between overriding and subducting plate, and leads to cessation of subduction. This hydration is mainly the result of dewatering of serpentine and metabasalts in the subducting slab. Slab dewatering probably occurs generally between 50 - 200 km (Schmidt and Poli, 1998; Rüpke et al., 2004). Mantle wedge hydration is therefore likely to occur over the full potential temperature range $T_{pot} = 1350 - 1650^o$C considered here. Even though the importance of mantle wedge hydration weakening is less important for a hotter Earth, in which the mantle wedge is already intrinsically weak due to temperature dependent rheology, we decided to include this feature in all models. To that end, we define a region of 150 km wide and 40 km deep below the continent above the subducting slab where the effective viscosity is lowered by a factor 10 or 100 (see Figure 1).

Experimental studies have shown that the dehydration of fertile mantle material during the first few percentages of melt extraction can cause a significant increase in the effective strength of the residual harzburgite (Hirth and Kohlstedt, 1996). We therefore applied one set of models with a 100-fold stronger depleted harzburgite layer. Since we already use the dry rheologies in (Karato and Wu, 1993), this factor 100 can be regarded as an upper bound.

2.3 Modeling procedure

Ideally, the examination of plate tectonics in a hotter Earth includes the initiation of subduction by creation of a new convergence zone. This process is clearly distinct from continuing subduction (Cloetingh et al., 1984; Toth and Gurnis, 1998; Regenauer-Lieb et al., 2001; Hall et al., 2003). Here, we restrict ourselves to situations in which the subduction zone has already developed. We can regard viable subduction in this situation as a minimum requirement for succesful plate tectonics: if subduction doesn't survive under these fully developed conditions, we don't need to worry about dynamically and rheologically more complex subduction initiation in this setting either. To that end, we start each calculation with a kinematic phase, in which we temporarily force a v_{subd} cm/yr subduction velocity on an oceanic plate. Kinematic driving of subduction is continued until the tip of the slab has reached a depth of 200 km. We use this situation as a starting point for 'free' subduction (i.e. buoyancy driven without an imposed subduction velocity).

Long calculation times prohibit reaching a statistical steady state temperature profile. Especially the calculations with a high potential temperature T_{pot} show extremely rapid fluid motions that limit the acquired model time span of the calculation. A self-consistent model should, however, have an oceanic plate temperature distribution that roughly corresponds to the half-spreading velocity, and therefore also (because of our fixed MOR-trench distance) to the subduction velocity. The reason is that this distribution influences the thermal buoyancy forces that drive subduction, and therefore influences the subduction velocity. To varify this model characteristic, we check a posteriori if the average subduction velocity within a given model time window is consistent with the initially imposed one to which the oceanic temperature profile corresponds. The increased effective Rayleigh number of the higher T_{pot} calculations reduces the characteristic temporal and spatial dimensions of the dynamical processes. We found that for $\Delta T_{pot} = 0$, 100, 200, and 300K, an averaging window of 20, 10, 5, and 2.5 Ma was sufficiently long, and still numerically feasible. This a posteriori check leads to an iterative modeling approach: if initial and resulting average subduction velocity profile do not correspond, new calculations with different initial subduction velocity are examined, until initial and average velocities match close enough. Since subduction velocity variations occur (both in our modeling and in the real Earth), we take a rather 'loose' convergence criterion here, and require that the two plate velocities should differ by no more than 5 cm/yr. This usually limits the number of iterations to 3 or 4.

Even for today's subduction, many rheological and petrological model parameters (such as yield stress, crustal strength, fault friction, and basalt-to-eclogite transition speed) are poorly known. But those parameters can influence the subduction process significantly. Therefore, we performed model calculations for a range of parameter settings. One clear and obvious constraint for all models is that it should produce a 'reasonable' subduction process under today's conditions, i.e. with the present-day potential temperature and crustal thickness. A 'reasonable' model is assumed to show buoyancy-driven subduction velocities between 5 and 10 cm/yr. Parameter combinations that fail to do so are exempt from further investigation. Successful combinations are examined for hotter-Earth conditions.

3 Model results

3.1 Effect of potential temperature

In a first set of experiments, we show the effect of an increased mantle potential temperature difference ΔT_{pot} with respect to the present-day value (assumed to be 1350^{o}C). We increased ΔT_{pot} from 0 K up to 300 K in steps of 100 K. We use the following default parameters for these calculations, and varied those parameters in later calculations:

- crustal dislocation creep rheology from Shelton and Tullis (1981)
- an overall yield stress $\tau_y = 200$ MPa
- basalt-to-eclogite complete transformation in 1 Ma
- a free-slip subduction fault
- a hydrated mantle wedge that has a 100 times lower effective viscosity than 'normal' mantle under the same circumstances
- the depleted mantle residue after MOR melt extraction has the same rheology as fertile mantle material.

Figure 2 shows the results for subduction under these default parameter settings for different T_{pot}. The present-day situation (ΔT_{pot} = 0K or T_{pot} = 1350^{o}C) shows a slowly starting subduction process: little slab pull is available from the initially short slab. But as the slab length increases, subduction becomes progressively faster. It reaches a peak value when penetrating the 400-D phase transition. After that, it slows down, and starts to accumulate in the transition zone (between 400 and 670 km depth). The $\Delta T_{pot} = 100$K case shows the same characteristics as the $\Delta T_{pot} = 0$K case, but a few differences can be observed:

- The average subduction velocity is approximately twice as high as in the $\Delta T_{pot} = 0$K case, and correspondingly the plate is younger and thinner when arriving at the trench.
- The higher T_{pot} and correspondingly weaker mantle result in a more vigorous and chaotic convective instability. This is visible in the slightly more irregular subduction velocity.
- the slab doesn't penetrate into the lower mantle. This issue will be discussed below.

For $\Delta T_{pot} = 200$K, the slab breaks into pieces at a depth of around 200 km. Apparently, the slab is much weaker than in a cooler mantle. This 'slab detachment' results in large peaks in the subduction velocity, but doesn't significantly hamper the subduction process: the average subduction process is still around 20 cm/yr. The detached slab pieces all settle at the bottom of the transition zone, above the 670-km discontinuity. For the $\Delta T_{pot} = 300$K, slab detachment occurs at very shallow depth within the first Ma. After that, no slab pull exists anymore to drive the subduction process, and subduction ceases completely after 2 Ma. Whether it will re-appear when the slab is old enough or not depends on the amount of work needed to bend the plate that is increasingly thickening with age.

3.2 Effect of yield stress

One of the less well known rheological parameters is the yield stress τ_y. Our default value was rather arbitrarily chosen to be $\tau_y = 200$ MPa. In a first experiment, we reduce τ_y to 100 MPa. Figure 3 shows the resulting effect on the subduction dynamics for different mantle temperatures. For $\Delta T_{pot} = 0$ and 100K, this difference with the default model in section 3.1 is small: the reduced τ_y still does not lead to any slab break-off. For the $\Delta T_{pot} = 200$K case, slab breakoff is somewhat more frequent, and somewhat more shallow than in the default case. This results in a lower average subduction velocity of 15 cm/yr (versus 20 cm/yr in the default case). For the $\Delta T_{pot} = 300$K case, a different style of slab breakoff leads to more effective subduction than in the default case: because the break-off is less shallow, it doesn't stop subduction completely, but its rather frequent occurrence (once every 0.75 Ma in this case) only slows it down.

We also performed calculations with larger values of the yield stress: $\tau_y = 400$ MPa (results not shown) and 1 GPa (Figure 4). Such large yield stresses are probably representative for Peierl's creep as the stress-limiting deformation mechanism (Karato, 1996; Kameyama et al., 1999; Karato et al., 2001; Čížková et al., 2002). Two effects of the larger yield stress can be observed. For the lower mantle temperatures ($\Delta T_{pot} \leq 100$K), the higher yield stress gives rise to larger bending stresses, and requires more work to bend the plate into the subduction zone. This leads to slower subduction. For higher mantle temperatures another effect dominates: the higher yield stress prevents frequent slab break-off, and gives on average longer slabs, and therefore more slab pull and higher subduction velocities. In summary, the general style and pattern in the different τ_y-models is not significantly different from the default case in Figure 2, but higher τ_y calculations show faster subduction in a hotter Earth, because slabs are stronger, and don't break very easily.

3.3 Effect of plate coupling

At shallow depths, the coupling between overriding and subducting plate is determined by the fault friction. Below this fault (in our models at a depths greater than 100 km) the viscosity of the subducting oceanic crust and mantle wedge determine the intraplate coupling. We varied both coupling mechanisms to investigate their effect on the subduction process.

The effect of a non-zero fault friction is shown in Figure 5. In these calculations, a linear fault friction (the tangential shear stress is taken proportional to the slip velocity) of 1 MPa for every cm/yr slip velocity is imposed. For a 5 cm/yr slip velocity, this adds up to 5 MPa, a value that corresponds to the value found by Zhong and Gurnis (1992). For $\Delta T_{pot} = 0$ and 100 K, the peak in the subduction velocity upon penetration of the 400-km discontinuity is significantly reduced, but the overall effect is otherwise quite small. For higher ΔT_{pot}, a very regular subduction pattern appears, with slab detachments every 2.5/1.25 Ma for $\Delta T_{pot} = 200$ and 300 K, respectively. The average subduction velocity for these last two cases is reduced with respect to the default case in Figure 2. Model calculations are also performed for a higher fault friction case of 30 MPa for a 5 cm/yr subduction, which corresponds to the upper limit proposed by Zhong and Gurnis (1994). Results are not shown in a figure, but the main characteristics of those calculations are that in all but the present-day case, slab detachment occurs when the subducting plate reaches the 400-D continuity: the strong slab pull force of the 400-D discontinuity on the slab plus the strong resisting force from the fault friction causes a large tensional stress that tends to break off the slab in the hotter Earth cases where the slab is relatively hot and weak. For this high fault friction case, average subduction velocity remains low throughout the whole potential temperature range, considered here.

In the default model setup, the 100 times weaker-than-normal hydrated mantle wedge enables decoupling below the fault depth. Here we investigate if this decoupling role can be partly accomplished by weaker subducting oceanic crust. To that end, we increased the strength of the mantle wedge by a factor 10, and reduced the strength of the oceanic crust by changing its rheological prefactor with 6 orders of magnitude, which has the net effect of reducing in the effective crustal viscosity by approximately a factor 100. Results are shown in Figure 6. For all mantle temperatures, a general effect is observed: once heated up in the mantle, the crustal material becomes so weak that it separates from the mantle part of the slab. Since this crust is predominantly in the eclogitic phase, and therefore denser than mantle material, this implies that this separation removes a lot of the available slab pull from the slab. For $\Delta T_{pot} = 0$ and 100K, this effect is rather small, and the subduction velocity is almost the same as in the default case. Pieces of delaminated crust, however, are clearly visible just below the 400 km phase boundary in the lowermost panels of these cases. But for the significantly thicker crust in the $\Delta T_{pot} = 200$K this effect is larger, and slows down considerably the subduction process. For the highest potential temperature case, in which case most of the lithosphere is restricted within the thick weak crust, very frequent break-off, almost continuous dripping of the slab is observed. In this case, no coherent subducting slab is present, and analogy with present-day subduction is almost absent.

3.4 Effect of the basal-to-eclogite phase change kinetics

As illustrated above, the crustal phase transition of basalt to eclogite provides an important increase in the driving force behind subduction. Without this transition, the thick crust created by pressure release partial melting in a hot mantle would be too buoyant to subduct (Vlaar and van den Berg, 1991; Davies, 1992), analogous to present-day continental lithosphere. It is therefore expected that the kinetics of this transition play an important role in the subduction dynamics. Here, we examine this role by changing the (default) kinetics (full transition within 1 Ma) to 5 Ma (Figure 7). Rubie (1990), Hacker (1996) and Austrheim (1998) showed that hydration is expected to influence the eclogitization dynamics significantly. Most oceanic floor is probably hydrated to some extent and some depth, so we expect this 5 Ma slow kinetic rate to be an upper limit.

In this slow kinetics case (Figure 7), the preservation of crust in the light, basaltic phase significantly reduces the available slab pull to drive subduction, which leads to a slower subduction for all mantle temperature cases. But the effect is larger for the higher mantle temperature cases, where the crust is thicker: for the $\Delta T_{pot} = 200$K case, the reduction in subduction velocity is approximately a factor 2. For the $\Delta T_{pot} = 300$K case, subduction starts only very slowly: subduction can only be as quick as the transition to eclogite is.

3.5 Effect of a strong depleted MOR melt residue

Sofar all models assumed that MOR melt extraction doesn't change the rheology of the residue. The dehydration during melt extraction will probably strengthen the material. This is partly already compensated for by using the 'dry' rheology from Karato and Wu (1993). However, this strengthening can be much larger (Hirth and Kohlstedt, 1996), and rheological layering may have some dynamical influence on the slab morphology. Based on parameterized convection models, Korenaga (2005) suggests that this dehydration strengthening has a large effect on the dynamics of plate tectonics, as it slightly slows down plate tectonics instead of speeding it up for an increasing mantle temperature. Therefore, we present a set of calculations in which the depleted MOR melt residual layer (or shortly harzburgite layer) is a 100 times stronger than fertile material. Figure 8 shows the resulting subduction dynamics. Especially for the high ΔT_{pot} cases, where the harzburgite layer is thick, the rheological thickness of the plate is significantly increased with respect to the default case. The stronger harzburgite layer requires more bending energy which slows down subduction in comparison to the default case for $\Delta T_{pot} \leq 200$K. Another effect, however, is that the stronger harzburgite layer prevents slab breakoff, even for the $\Delta T_{pot} = 300$K case, which speeds up the subduction process. The harzburgite thickness increases with T_{pot}, and one would expect that bending of this increasingly thicker layer would result in lower subduction velocities v_{subd}, similar to the findings of Korenaga (2005). However, the opposite is observed: v_{subd} increases with T_{pot}, because the weakening effect of increasing T_{pot} (in both lithosphere and underlying mantle) dominates over the thickening effect of the harzburgite layer.

4 Discussion

4.1 Subduction velocity and viability

We compiled the subduction velocities of all performed calculations (Figure 9), averaged over a suitable time window (Section 2.3). Each calculation has an uncertainty in the subduction velocity of 5 cm/yr. This is the allowed discrepancy between the initially imposed subduction velocity v_{ini} and the (a posteriori determined) average subduction velocity v_{subd}, and should be regarded as the natural relatively short-term variation in subduction velocity (short-term with respect to secular cooling, i.e. Ma, not Ga timescale). Most cases have a v_{subd} of 5, 10, 15, or 20 cm/yr, because one of those values have a close enough match with the initially imposed velocity v_{ini}. In some calculations, however, v_{subd} depends strongly on v_{ini}, and in those cases further iterations were necessary.

Although each model has its own characteristic average subduction velocity v_{subd} as a function of potential temperature T_{pot}, a general pattern can be recognized amongst most models. Almost all models show an increase in v_{subd} if ΔT_{pot} is increased from 0 to 100K, and maximum v_{subd} is observed for most models at $\Delta T_{pot} = 100$ or 200K. For higher T_{pot} v_{subd} often reduces again. Increasing v_{subd} with mantle temperature for the lower ΔT_{pot} models indicates that the hotter mantle facilitates the subduction process, most likely as a result of the weaker mantle, and the smaller bending energy required for subduction. A decrease of v_{subd} with mantle temperature for the higher ΔT_{pot} models indicates that the hotter mantle resists subduction more: subduction-resisting effects become more important. Those resisting effects are 1) lithospheric buoyancy, and 2) slab weakness, slab breakoff, and crustal decoupling from the mantle lithosphere. Both factors reduce the effective slab pull, which results in slower subduction rates. However, results from the model with stronger harzburgite or high yield stress show continued subduction velocity increase with increasing T_{pot}, and slab breakoff does not occur or occurs less. This indicates that slab breakoff is the dominant factor reducing the subduction vigor in a hotter Earth. However, during initiation of subduction (a situation circumvented due to our modeling procedure), the resisting effect from lithospheric buoyancy may be more dominating than for fully developed slabs as studied here.

To give an overview of the effects of different physical parameters, Figure 10 summarizes the style of subduction as a function of varied physical parameter and mantle temperature. This plot clearly shows that for $\Delta T_{pot} = 100$K, subduction still appears a very viable and robust mechanism, independent of physical parameter settings. For $\Delta T_{pot} = 200$K, most calculations show slab detachment, but the cases with a relatively strong slabs ($\Delta\eta_{Hz} = 100$) or slow (and therefore old and strong) slabs ($f_f = 30$ MPa and slow b$\rightarrow$e) still show subduction that resembles the present-day situation. For $\Delta T_{pot} = 300$K, some cases show no subduction at all anymore.

This result puts some earlier ideas on the viability of subduction in the early Earth in a different light. One idea was based on the concept that buoyancy considerations limit the viability of subduction in a hotter Earth (Vlaar and van den Berg, 1991; Davies, 1992; Abbott et al., 1994; van Thienen et al., 2004c). These buoyancy considerations may be important for starting subduction, when no slab is yet present. But the calculations shown here show that eclogitization during developed subduction is capable to keep subduction going, even if the crust and harzburgite layers are thick.

Some models show roughly present-day subduction velocities throughout the whole potential temperature range considered. In these models, factors such as slow eclogitization and large intraplate contact friction limit the subduction rates. These factors are independent of T_{pot} in our models (although not necessarily in the real Earth), and therefore subduction velocity is also more or less independent of T_{pot}. Those models suggest that the subduction process, and possibly also plate tectonics, continued throughout the Earth's history with roughly the present-day appearance, although possibly with with more frequent slab breakoff.

4.2 Relation to the occurrence of UHP metamorphism

Most eclogites are not older than about 600 MPa (Maruyama and Liou, 1998; Jahn et al., 2001), and most blueschists facies metamorphism date back to about 800 Ma (Maruyama and Liou, 1998). This lack of old ultra-high-pressure metamorphism (UHPM) is mostly attributed to secular cooling of the Earth and associated change in geothermal gradient. This could have led to an increase of plate thickness and slab pull (Miyashiro, 1981) and changed pT conditions (Maruyama and Liou, 1998). Möller et al. (1995) found evidence for 2-Ga-old eclogites, and their combined evidence suggests that those eclogites originate in a subduction setting. They speculated that absence of UHPM could be a preservation problem. Stern (2005) recently contributed to this discussion by suggesting that the absence of UHPM prior to the Neoproterozoic is a result of excess buoyancy of oceanic lithosphere (Vlaar, 1986; Vlaar and van den Berg, 1991; van Thienen et al., 2004c) that prevents collapsing into the underlying asthenosphere. But our model results show that including the basalt-to-eclogite transition of oceanic crust significantly reduces this buoyancy effect, unless very slow eclogitization kinetics are assumed. The presented model results put forward a new explanation for the occurrence of (UHP) metamorphism through geological time: absence of UHP metamorphic rocks prior to the late Precambrian can be related to a secular change in the rheological strength of subducting slabs.

A commonly accepted mechanism for the creation and exhumation of UHPM rocks is subduction of continental crust during continental collision to dehydrate and recrystallize into blueschists and eclogites at shallow depths, or even coesites and diamonds at greater depths (Liou et al., 1998; van Roermund et al., 2002; Spengler et al., 2006). The overall buoyancy of the continental crust, possibly aided by breakoff of the denser, deeper part of the slab (Davies and von Blanckenburg, 1998) is likely to be responsible for the exhumation of the UHP rocks. Grambling (1981) shows that average metamorphic geotherms have decreased throughout the Earth's history. This is commonly attributed to the decreasing mantle temperature due to secular cooling of the Earth. But Grambling also shows that average metamorphic pressures have increased since the Earth's early history. Apparently, prior to the late Precambrian, tectonic conditions were unfavorable to deeply subduct crustal rocks. Most of our model results show that in a 200-300 K hotter mantle, slabs have an increased tendency to break off whenever tensional stresses are too large (Figure 10. When oceanic subduction is followed by continental subduction, tensile stresses are large, because the dense oceanic lithosphere applies a slab pull, while the buoyant continental lithosphere tries to resist subduction. Related to the ideas by Davies and von Blanckenburg (1998), we hypothesize that in a hotter Earth slab detachment occurred soon after arrival of continental lithosphere at the trench. This slab detachment will stop any further subduction, and continental rocks never reach UHP conditions. In other words, strong slabs are necessary to drag down continental rock to UHP conditions, and slabs were not strong in a hotter Earth. Note that our hypothesis, just like the model by Stern (2005), presents an explanation for the late occurrence of UHPM, but it doesn't necessarily require absence of subduction prior to UHPM, but merely absence of continental subduction. It is, however, likely that the style of earlier subduction was quite different from the subduction process we know today, and our model results (e.g. Figure 2) confirm this.

4.3 Cooling history of the Earth

The wide variety in both observations and theoretical models suggest that the cooling history of the Earth is still rather uncertain. We could start from the assumption that the Earth has been cooling at a constant pace. In that case, the higher heat productivity by radioactive decay in the early Earth required more effective cooling of the planet through its surface: estimates for the Archean suggest a heat production that is 2 to 3 times higher than today (Sleep, 2000; Turcotte and Schubert, 2002). Total heat flow through the oceanic lithosphere is proportional to the mantle potential temperature, and inversely proportional to the square root of the average lifetime of the oceanic plates (Sleep, 2000):

$$\frac{q_p}{q_{p0}} = \frac{T_L}{T_{L0}}\sqrt{\frac{t_{p0}}{t_p}} \tag{9}$$

where q_p is the total heat flow, T_L the mantle potential temperature, t_p the average maximum age of the plate, and the subscript 0 refers to today's situation. This implies an approximately 3 to 7 times younger lithosphere for a 200K warmer mantle. We can use the above calculation to predict for each model its ability to cool a younger Earth at its present-day cooling rate. If we assume an average present-day plate age of 120 Ma upon subduction (Turcotte and Schubert, 2002), the Archean plates should have been only 17 to 40 Ma old at the trench, which implies that our (rather short) oceanic plate should subduct with about 7 to 15 cm/yr to maintain a surface heatflow that can compete with the radioactive heat production to maintain the Earth' present-day cooling rate. Note, however, that these required plate velocities increase linearly with the length of the oceanic plate, and that they are slightly dependent on the mantle temperature. Nonetheless, the age of the plate and therefore also its strength, one of the major controls in the viability of Archean subduction, is independent on the ridge-trench distance. Comparing those required subduction velocities with those from the model calculations in Figure 9 suggest the following:

1. None of the calculations show average subduction velocities that are much larger than the 7 - 15 cm/yr to maintain the present-day cooling rate. This indicates that a 'thermal catastrophe' as predicted from some Q-Ra models is not expected.

2. Most models with $\Delta T_{pot} = 100$K have subduction velocities that are large enough to maintain the present-day cooling rate. But for $\Delta T_{pot} = 200$ or 300K, the calculations with fault friction, and possibly the default calculation and the one with slow eclogitization kinetics could be too slow for that. Such models predict that the early Earth has been cooling at a slower pace than today, and its initial potential temperature may not have been very different from today's value. van Thienen et al. (2005) showed that such slow plate tectonics could still be sufficient to cool the Earth. The other models show subduction velocities that roughly fall within the

7-15 cm/yr range calculated above, and could be taken as an indication that the Earth indeed followed an average cooling rate that is not too different from today's cooling rate.

3. The peak velocities around ΔT_{pot} = 100 - 200K (or T_{pot} = 1450 - 1550^{o}C) in most models suggest that the Earth was cooling fastest for those mantle temperatures.

For all the above speculations on the Earth's cooling rate, however, we have to keep in mind that the uncertainty in many model parameters is still large. Also the inability to run model calculations until statistical steady state is reached limits the applicability of these models to the cooling history of the Earth: cooling rates cannot be inferred directly from our model calculations. Furthermore, no tectonic mechanism other than plate tectonics is considered here. Addition of other mechanisms would obviously change the results (van Thienen et al., 2005). Future improvements in these directions will narrow the uncertainty range on the Earth's cooling history.

4.4 Phase transitions in a 2-D model

All presented model calculations show a sharp peak in the subduction velocity when the tip of the slab penetrates the 400-km discontinuity. Such peak velocity is unlikely to occur in the real Earth. The main cause for this peak is the two-dimensionality of the model: since no lateral changes (i.e. in the third dimension) in the slab can occur, all parts of the slab reach the 400-km discontinuity at the same time, leading to a strong, sudden increase in the driving force of the subduction process. As a consequence, the occurrence of slab detachment during this initial penetration would be less abundant in a 3-D model. For similar reasons initial penetration through the 670-km discontinuity is more difficult in a 2-D model: without any variation in the third dimension, all parts of the slab in that direction are forced to penetrate this discontinuity at the same time, which requires a concentrated amount of energy that might not be available. There is, however, another, physical explanation for the lack of slab penetration in higher potential temperature models: the (thicker) eclogitic crust is buoyant below the 670-km discontinuity (which only applies to mantle material), and so crust is stably stratified at this depth (van Keken et al., 1996; Karato, 1997). This buoyancy effect was larger in an early Earth when the crust was thicker.

4.5 Slab detachment

In the ΔT_{pot} = 300K experiments, events of crustal decoupling or detachment of slab material dominate and eventually terminate subduction in several of the presented models. Although different in frequency and size, these processes show some similarities with slab detachment, as suggested to occur today in three-dimensional settings in final stages of a subduction process, for example at the closure of an oceanic basin (Wortel and Spakman, 2000). Negative convergence velocities (not shown in the figures) can be associated with geologically and numerically observed surface uplifts after slab detachment (Davies and von Blanckenburg, 1995; van der Meulen et al., 2000; Buiter, 2000; Gerya et al., 2004).

4.6 Effects from hydration and melting

One of the main indications for a higher Archean mantle temperature comes from high-MgO komatiites found in Archean greenstone belts. It has been suggested that the presence of water can explain komatiite formation at much lower temperatures than previously thought (i.e. a wet instead of a hot Archean mantle). The actual geodynamical differences between a hotter and a wetter mantle may not have been very large. The reason for that is that both an increased temperature and an increased degree of hydration have similar effects in all the influencing physical parameters of this study. The mantle viscosity decreases with about an order of magnitude for every 100 K temperature increase, but the effect of increased hydration is quite comparable (Mei and Kohlstedt, 2000a,b; Karato and Jung, 2003). The average thickness of oceanic crust and harzburgite layers increase with increasing mantle temperature (Vlaar and van den Berg, 1991), but the presence of water significantly lowers the mantle solidus (Kawamoto and Holloway, 1997), which may lead to a similar effect. The question is whether the mantle is hydrated enough for these effects to be significant. Also eclogite formation kinetics increases with both temperature and water content (Rubie, 1990; Hacker, 1996; Austrheim, 1998), and, although these effects are not well quantified, they are qualitatively probably rather similar. We parameterized the different physical circumstances in a younger Earth through temperature increase, but maybe the geodynamical consequences could be rather similar for a more modest temperature increase in combination with an increased water content. Better quantification of such analogy is necessary and are part of future research planned.

Although its implications are partly parameterized in these models, melting processes are not explicitly present in our numerical simulations. Crustal melting in hotter subduction zones, especially during episodes of slab breakoff, could lead to different buoyancy distributions and effective slab pull, and the expected difference in the composition of the arc volcanism could be used to further relate model results to field observations. A common material found in granite-greenstone terrains in Archean cratons is Tonalite-Trondhjemite-Granodiorite (TTG) (Goodwin, 1991), and conditions for the formation of TTGs are probably met in Archean subduction zones (Rapp et al., 1991), but alternative tectonic settings have been suggested (Smithies, 2000; van Thienen et al., 2004a). Melt extent and composition at MORs is dependent not only on the mantle temperature, but also the degree of depletion of the upper mantle by former melting and remixing of subducted slab material, and a secular change in the degree of mantle depletion could have a non-negligible effect on the composition, density, and rheology of both the melt (MORB) and its residue (harzburgite) (van Thienen et al., 2004c). Furthermore, a changing rheology due to the presence of large amounts of melt could have a profound influence on the slab strength and subduction dynamics, and its effect should be taken into account in future model improvements.

5 Conclusions

To investigate the quantification of the tectonic characteristics of the Precambrian Earth, we studied the subduction process in a hotter mantle with numerical model calculations. Results indicate that the viability and 'mode' of the plate tectonic mechanism in a hotter Earth is determined by a complicated interaction between crustal thickness, eclogitization rate, and the rheology of both crust and mantle. For a mantle temperature increase of 100 K, we find subduction to be essentially the same as today, although faster. In a hotter mantle frequent events of crustal separation and detachment significantly alter and sometimes hamper subduction. Increasing the yield strength (the maximum stress the slab can resist) has two opposing effects: 1) the subduction process consumes more bending power, which makes the subduction process slower. This effect dominates for $\Delta T_{pot} \leq$ 100K, and 2) more slab coherency avoids frequent slab break-off and allows longer slabs to enable faster subduction. A modest amount of fault friction has little influence for today's subduction other than slowing down the plate motion. In a younger Earth, it could have had a stabilizing effect by avoiding either shallow break-off and subsequent blocking of the subduction process, or preventing periods of rapid subduction, as observed in calculations without fault friction. The hydrated mantle wedge should be weak enough (about a factor 100 weaker than normal mantle material to allow for enough decoupling of the converging plates below the depth of the overriding lithosphere. Instead, a very weak subducting oceanic lithosphere can also perform this decoupling role. The consequence of that, however, is that this weak crustal material can easily separate from the rest of the slab, once entering the hot mantle and heating up, and this process significantly influences the available slab pull force. This effect is larger for a higher ΔT_{pot} in which case the crust is thicker. The kinetics of eclogitization play an important role for subduction in the past: a complete transformation period of 1 Ma is fast enough to allow for rapid subduction, even for a thick crust. If this transformation period is as long as 5 Ma, subduction will be very slow for higher ΔT_{pot}. Finally a strong harzburgite layer prevents slab breakoff and leads to faster subduction relative to the other models.

For none of the explored model parameter combinations, average model subduction velocities show an exponential increase with mantle temperature. Therefore, unlike some parameterized convection models suggest, extrapolation of the present tectonic regime to a hotter Earth is not creating a 'thermal catastrophe'. Instead, subduction velocity in a hotter mantle range from slightly lower than today up to a few times faster than today. This suggests that past cooling of the Earth has been about as fast or slower than today.

Even though subduction seems viable under certain parameter settings, the limited strengths of the slab and in particular the crust probably resulted in a different style of subduction, in which frequent slab breakoff and possibly crustal delamination played a more dominant role. We hypothesize that this reduced strength hampers carrying continental crust to eclogite- or even blueschist conditions, and that this is the main reason for the absence of UHPM prior to the late Precambrian.

Acknowledgments

Greg Houseman and an anonymous reviewer are thanked for their constructive comments on this manuscript. Furthermore, we would like to thank Taras Gerya and Herman van Roermund for very stimulating discussions.

References

Abbott, D., Drury, R., and Smith, W. H. F. (1994). Flat to steep transition in subduction style. *Geology*, 22:937–940.

Ahrens, T. J. and Schubert, G. (1975). Gabbro-eclogite reaction rate and its geophysical significance. *Rev. of Geophysics and Space Physics*, 13(2):383–400.

Austrheim, H. (1998). Influence of fluid and deformation on metamorphism of the deep crust and consequences for the geodynamics of collision zones. In Hacker, B. and Liou, J., editors, *When continents collide: geodynamics and geochemistry of ultrahigh-pressure rocks*, pages 297–323. Kluwer academic publishers.

Billen, M. I. and Gurnis, M. (2001). A low viscosity wedge in subduction zones. *Earth Plan. Sci. Let.*, 193:227–236.

Bina, C. and Helffrich, G. (1994). Phase transition Clapeyron slopes and transition zone seismic discontinuity topography. *J. Geophys. Res.*, 99(B8):15853–15860.

Buiter, S. J. H. (2000). *Surface deformation resulting from subduction and slab detachment.* PhD thesis, Utrecht Univ., The Netherlands.

Christensen, U. R. and Yuen, D. A. (1985). Layered convection induced by phase transitions. *J. Geophys. Res.*, 99:10291–10300.

Cížková, H., van Hunen, J., van den Berg, A. P., and Vlaar, N. J. (2002). The influence of rheological weakening and yield stress on the interaction of slabs with the 670-km discontinuity. *Earth Plan. Sci. Let.*, 199:447–457.

Cloetingh, S. A. P. L., Wortel, M. J. R., and Vlaar, N. J. (1984). Passive margin evolution, initiation of subduction and the Wilson cycle. *Tectonophysics*, 109:147–163.

Conrad, C. P. and Hager, B. H. (2001). Mantle convection with strong subduction zones. *Geophys. J. Int.*, 144:271–288.

Davies, G. F. (1992). On the emergence of plate tectonics. *Geology*, 20:963–966.

Davies, J. H. and von Blanckenburg, F. (1995). Slab breakoff: a model of lithospheric detachment and its test in the magmatism and deformation of collisional orogens. *Earth Plan. Sci. Let.*, 129:85–102.

Davies, J. H. and von Blanckenburg, F. (1998). Thermal controls on slab breakoff and the rise of high-pressure rocks during continental collisions. In Hacker, B. R. and Liou, J. G., editors, *When continents collide: geodynamics and geochemistry of ultrahigh-pressure rocks*, pages 97–115. Kluwer Acedamic Publishers.

de Wit, M. J. (1998). On Archean granites, greenstones, cratons and tectonics: does the evidence demand a verdict? *Precambrian Res.*, 91:181–226.

England, P. and Bickle, M. (1984). Continental thermal and tectonic regimes during the Archaean. *Journal of Geology*, 92:353–367.

Gerya, T. V., Yuen, D. A., and Maresch, W. V. (2004). Thermomechanical modelling of slab detachment. *Earth Plan. Sci. Let.*, 226:101–116.

Goodwin, A. M. (1991). *Precambrian Geology.* Acedamic Press, London.

Grambling, J. A. (1981). Pressures and temperatures in Precambrian metamorphic rocks. *Earth Plan. Sci. Let.*, 53:63–68.

Grigné, C., Labrosse, S., and Tackley, P. J. (2005). Convective heat transfer as a function of wavelength: Implications for the cooling of the earth. *J. Geophys. Res.*, 110:B03409, doi:10.1029/2004JB003376.

Hacker, B. R. (1996). Eclogite formation and the rheology, buoyancy, seismicity and H_2O content of oceanic crust. In *Subduction: Top to Bottom*, pages 337–346. AGU Monogr.

Hall, C. E., Gurnis, M., Sdrolias, Lavier, L. L., , and Muller, R. D. (2003). Catastrophic initiation of subduction following forced convergence at transform boundaries. *Earth Plan. Sci. Let.*, 212:15–30.

Hamilton, W. B. (1998). Archean magmatism and deformation were not products of plate tectonics. *Precambrian Res.*, 91:143–179.

Herzberg, C. (1992). Depth and degree of melting of komatiites. *J. Geophys. Res.*, 97:4521–4540.

Hirth, G. and Kohlstedt, D. L. (1996). Water in the oceanic upper mantle: implications for rheology, melt extraction and the evolution of the lithosphere. *Earth Plan. Sci. Let.*, 144:93–108.

Hoffman, P. F. and Ranalli, G. (1988). Archean oceanic flake tectonics. *Geophys. Res. Let.*, 15:1077–1080.

Irifune, T. and Ringwood, A. E. (1993). Phase transformations in subducted oceanic crust and buoyancy relations at depths of 600-800 km in the mantle. *Earth Plan. Sci. Let.*, 117:101–110.

Jahn, B., Caby, R., and Monie, P. (2001). The oldest UHP eclogites of the world: age of UHP metamorphism, nature of protoliths and tectonic implications. *Chem. geol*, 178:143–158.

Kameyama, M., Yuen, D. A., and Karato, S.-i. (1999). Thermal-mechanical effects of low-temperature plasticity (the Peierls mechanism) on the deformation of a viscoelastic shear zone. *Earth Plan. Sci. Let.*, 168:159–172.

Kanamori, H. (1980). The state of stress in the Earth's lithosphere. In Dziewonski, A. and Boschi, E., editors, *Physics of the Earth's interior*, pages 531–554. Amsterdam, North-Holland.

Karato, S.-i. (1996). Phase transformations and rheological properties of mantle minerals. In Crossley, D. and Soward, A. M., editors, *Earth's deep interior*, pages 223–272. Gordon and Breach Sci. Pub.

Karato, S.-i. (1997). On the separation of crustal component from subducted oceanic lithosphere near the 660 km discontinuity. *Phys. Earth Planet. Inter.*, 99:103–111.

Karato, S.-i. and Jung, H. (2003). Effects of pressure on high-temperature dislocation creep in olivine. *Philosophical Magazine*, 83(3):401–414.

Karato, S.-i., Riedel, M. R., and Yuen, D. A. (2001). Rheological structure and deformation of subducted slabs in the mantle transition zone: implications for mantle circulations and deep earthquakes. *Phys. Earth Planet. Inter.*, 127:83–108.

Karato, S.-i. and Wu, P. (1993). Rheology of the upper mantle: a synthesis. *Science*, 260:771–778.

Kawamoto, T. and Holloway, J. (1997). Melting temperature and partial melt chemistry of H_2O-saturated mantle peridotite to 11 Gigapascals. *Science*, 276:240–243.

Kohlstedt, D. L., Evans, B., and Mackwell, S. J. (1995). Strength of the lithosphere: Constraints imposed by laboratory experiments. *J. Geophys. Res.*, 100(B9):17587–17602.

Komiya, T., Maruyama, S., Masuda, T., Nohda, S., Hayashi, M., and Okamoto, K. (1999). Plate tectonics at $3.8 - 3.7$ ga: field evidence from the Isua accretionary complex, southern West Greenland. *Journal of Geology*, 107:515–554.

Korenaga, J. (2005). Archean geodynamics and the thermal evolution of Earth. to appear in AGU monograph on *Archean Geodynamic Processes*, December 2005.

Kukačka, M. and Matyska, C. (2004). Influence of the zone of weakness on dip angle and shear heating of subducted slabs. *Phys. Earth Planet. Inter.*, 141:243–252.

Kusky, T. M., Li, J.-H., and Tucker, R. D. (2001). The Archean Dongwanzi ophiolite complex, North China craton: 2.505-Billion-year-old oceanic crust and mantle. *Science*, 292:1142–1145.

Liou, J. G., Maruyama, S., and Cong, B. (1998). Introduction to geodynamics for high- and ultrahigh-repssure metamorphism. *Isl. Arc*, 7:1–5.

Maruyama, S. and Liou, J. G. (1998). Initiation of ultrahigh-pressure metamorphism and its significance on the Proterozoic-Phanerozoic boundary. *Isl. Arc*, 7:6–35.

Mei, S. and Kohlstedt, D. L. (2000a). Influence of water on plastic deformation of olivine aggregates 1: Diffusion creep regime. *J. Geophys. Res.*, 105:21457–21469.

Mei, S. and Kohlstedt, D. L. (2000b). Influence of water on plastic deformation of olivine aggregates 2: Dislocation creep regime. *J. Geophys. Res.*, 105:21471–21481.

Miyashiro, A. (1981). Tectonic and petrologic aspects of Asia. *Geol. Soc. China (Taiwan) Memoir*, 4:1–32.

Möller, A., Appel, P., Mezger, K., and Schenk, V. (1995). Evidence for a 2 Ga subduction-zone: Eclogites in the Usagaran belt of Tanzania. *Geology*, 23:1067–1070.

Parmentier, E. M. and Hess, P. C. (1992). Chemical differentiation of a convecting planetary interior: consequences for a one plate planet such as Venus. *Geophys. Res. Let.*, 20:2015–2018.

Peacock, S. M. (1993). The importance of blueschist → eclogite dehydration reactions in subducting oceanic crust. *Geol. Soc. Am. Bull.*, 105:684–694.

Philpotts, A. R. (1990). *Principles of igneous and metamorphic petrology.* Prentice Hall, New Jersey.

Rapp, R. P., Watson, B. E., and Miller, C. F. (1991). Partial melting of amplibolite/eclogite and the origin of Archean trondjemites and tonalites. *Precambrian Res.*, 51:1–25.

Regenauer-Lieb, K., Yuen, D. A., and Branlund, J. (2001). The initiation of subduction: criticality by addition of water? *Science*, 294:578–580.

Rubie, D. (1990). Role of kinetics in the formation and preservation of eclogites. In Carswell, editor, *Eclogite facies rocks*, pages 111–140. Blackie, Glasgow.

Rüpke, L., Morgan, J. P., Hort, M., and Connolly, J. (2004). Serpentine and the subduction zone water cycle. *Earth Plan. Sci. Let.*, 223:17–34.

Schmidt, M. and Poli, S. (1998). Experimentally based water budgets for dehydrating slabs and consequences for arc magma generation. *Earth Plan. Sci. Let.*, 163:361–379.

Schubert, G., Turcotte, D. L., and Olson, P. (2001). *Mantle convection in the Earth and planet.* Cambridge University Press.

Segal, A. and Praagman, N. P. (2005). The sepran fem package. Technical report, Ingenieursbureau Sepra, The Netherlands, http://ta.twi.tudelft.nl/sepran/sepran.html.

Shelton, G. and Tullis, J. (1981). Experimental flow laws for crustal rocks. *Eos, Trans. Am. Geoph. Union*, 62(17):396.

Sleep, N. H. (2000). Evolution of the mode of convection within terrestrial planets. *J. Geophys. Res.*, 105:17563–17578.

Smithies, R. H. (2000). The Archean tonalite-trondhjemite-granodiorite (ttg) series is not an analogue of cenozoic adakite. *Earth Plan. Sci. Let.*, 182:115–125.

Spengler, D., van Roermund, H. L. M., Drury, M. R., Ottolini, L., Mason, P. R. D., and Davies, G. R. (2006). Deep origin and hot melting of an archean orogenic peridotite massif in norway. *Nature*, 440:doi:10.1038/nature04644.

Stern, R. J. (2005). Evidence from ophiolites, blueschists, and ultrahigh-pressure metamorphic terranes that the modern episode of subduction tectonics began in Neoproterozoic time. *Geology*, 33:557–560.

Toth, J. and Gurnis, M. (1998). Dynamics of subduction initiation at preexisting fault zones. *J. Geophys. Res.*, 103(B8):18053–18067.

Turcotte, D. L. and Schubert, G. (2002). *Geodynamics, Applications of continuum physics to geological problems, Second Edition.* Cambridge University Press.

van den Berg, A. P., van Keken, P. E., and Yuen, D. A. (1993). The effects of a composite non-Newtonian and Newtonian rheology on mantle convection. *Geophys. J. Int.*, 115:62–78.

van der Meulen, M. J., Kouwenhoven, T. J., van der Zwaan, G. J., Meulenkamp, J. E., and Wortel, M. J. R. (2000). Late Miocene uplift in the Romagnan Apennines and the detachment of subducted lithosphere. *Tectonophysics*, 315:315–331.

van Hunen, J., van den Berg, A. P., and Vlaar, N. J. (2000). A thermo-mechanical model of horizontal subduction below an overriding plate. *Earth Plan. Sci. Let.*, 182:157–169.

van Hunen, J., van den Berg, A. P., and Vlaar, N. J. (2001). Latent heat effects of the major mantle phase transitions on low-angle subduction. *Earth Plan. Sci. Let.*, 190:125–135.

van Hunen, J., van den Berg, A. P., and Vlaar, N. J. (2004). Various mechanisms to induce present-day shallow flat subduction and implications for the younger earth: a numerical parameter study. *Phys. Earth Planet. Inter.*, 146:179–194.

van Keken, P. E., Karato, S., and Yuen, D. A. (1996). Rheological control of oceanic crust separation in the transition zone. *Geophys. Res. Let.*, 23(14):1821–1824.

van Roermund, H. L. M., Carswell, D. A., Drury, M. R., and Heijboer, T. C. (2002). Microdiamonds in a megacrystic garnet websterite pod from Bardane on the island of Fjrtoft, western Norway: Evidence for diamond formation in mantle rocks during deep continental subduction. *Journal of*

Geology, 30:959–962.

van Thienen, P., van den Berg, A. P., and Vlaar, N. J. (2004a). On the formation of continental silicic melts in thermochemical mantle convection models: implications for early Earth. *Tectonophysics*, 394:111–124.

van Thienen, P., van den Berg, A. P., and Vlaar, N. J. (2004b). Production and recycling of oceanic crust in the early Earth. *Tectonophysics*, 386:41–65.

van Thienen, P., Vlaar, N. J., and van den Berg, A. P. (2004c). Plate tectonics on the terrestrial planets. *Phys. Earth Planet. Inter.*, 142:61–74.

van Thienen, P., Vlaar, N. J., and van den Berg, A. P. (2005). Assessment of the cooling capacity of plate tectonics and flood volcanism in the evolution of Earth, Mars, and Venus. *Phys. Earth Planet. Inter.*, 150:287–315.

Vlaar, N. J. (1985). Precambrian geodynamical constraints. In Tobi, A. C. and Touret, J. L. R., editors, *The deep proterozoic crust in the North Antlantic provinces*, pages 3–20. Reidel.

Vlaar, N. J. (1986). Archaean global dynamics. *Geologie en Mijnbouw*, 65:91–101.

Vlaar, N. J. and van den Berg, A. P. (1991). Continental evolution and archeao-sea-levels. In Sabadini, R., Lambeck, K., and Boschi, E., editors, *Glacial Isostasy, Sea-Level and Mantle Rheology.* Kluwer.

Vlaar, N. J., van Keken, P. E., and van den Berg, A. P. (1994). Cooling of the Earth in the Archaean: Consequences of pressure-release melting in a hotter mantle. *Earth Plan. Sci. Let.*, 121:1–18.

Wortel, M. J. R. and Spakman, W. (2000). Subduction and slab detachment in the Mediterranean-Carpathian region. *Science*, 290:1910–1917.

Zegers, T. E. and van Keken, P. E. (2001). Middle archean continent formation by crustal delamination. *Geology*, 29:1083–1086.

Zhong, S. and Gurnis, M. (1992). Viscous flow model of a subduction zone with a faulted lithosphere: long and short wavelength topography, gravity and geoid. *Geophys. Res. Let.*, 19(18):1891–1894.

Zhong, S. and Gurnis, M. (1994). Controls on trench topography from dynamic models of subducted slabs. *J. Geophys. Res.*, 99(B8):15683–15695.

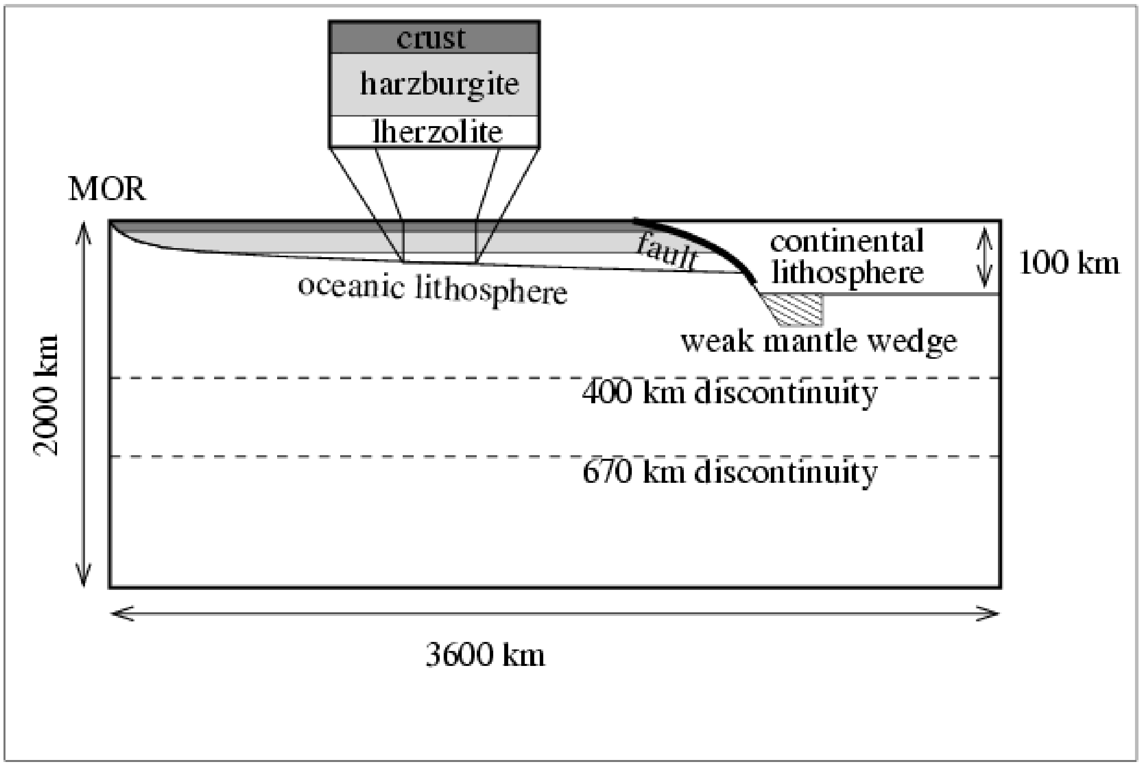

Figure 1: Schematic representation of the model setup.

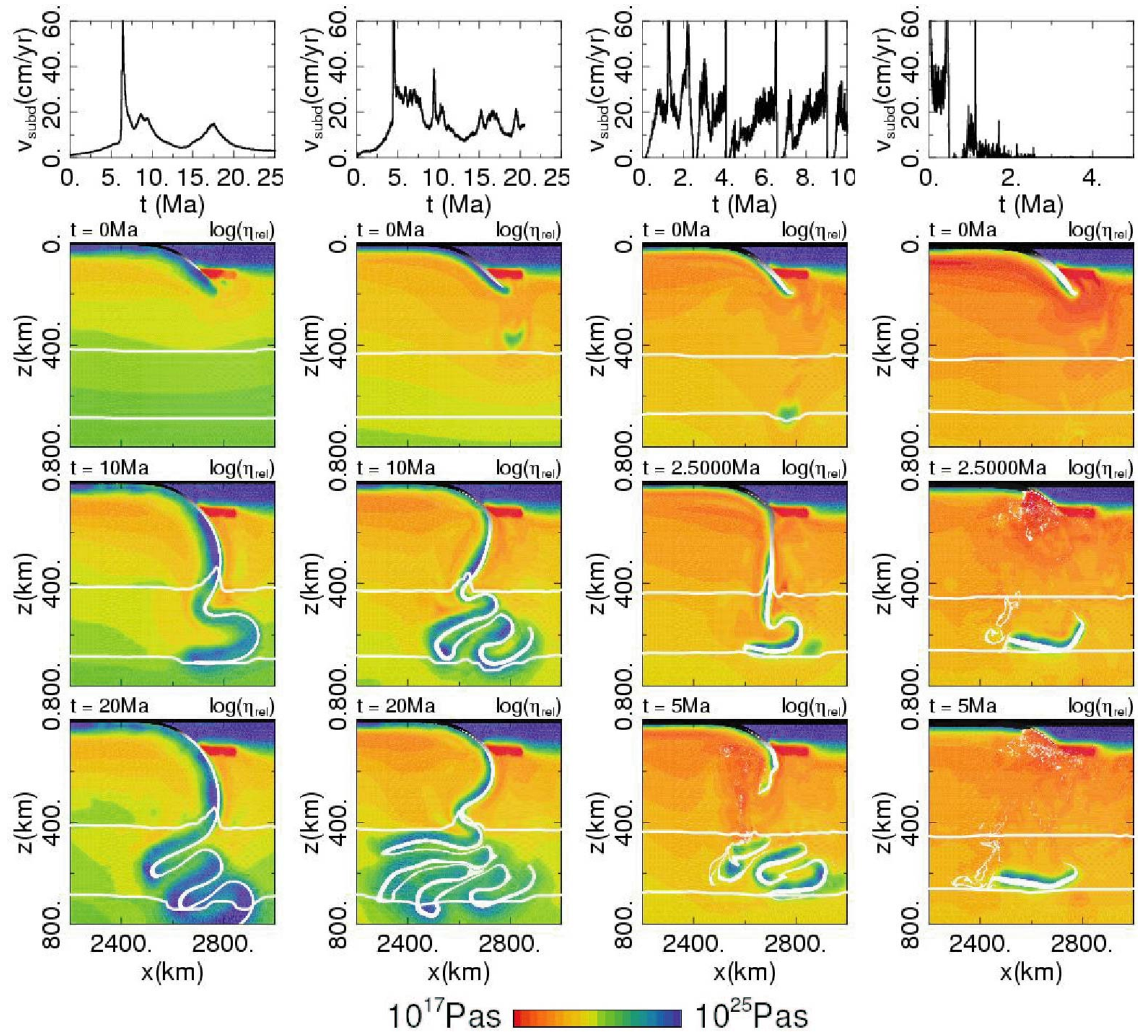

Figure 2: Top panel: Subduction velocity v_{subd} with respect to the overlying continent during the buoyancy-driven subduction process at a potential temperature increase ΔT_{pot} of a) 0K, b) 100K, c) 200K, and d) 300K above the present-day value. Default model parameters are used in these calculations (see text). The subduction process is initiated by a period of forced subduction. Time $t = 0$ refers to the transition from this forced subduction to free subduction. Lower three panels: time snapshots of the effective viscosity field for the subduction process. The olivine-spinel transition is denoted by the thin white line, crustal material by black areas, and eclogite by white areas.

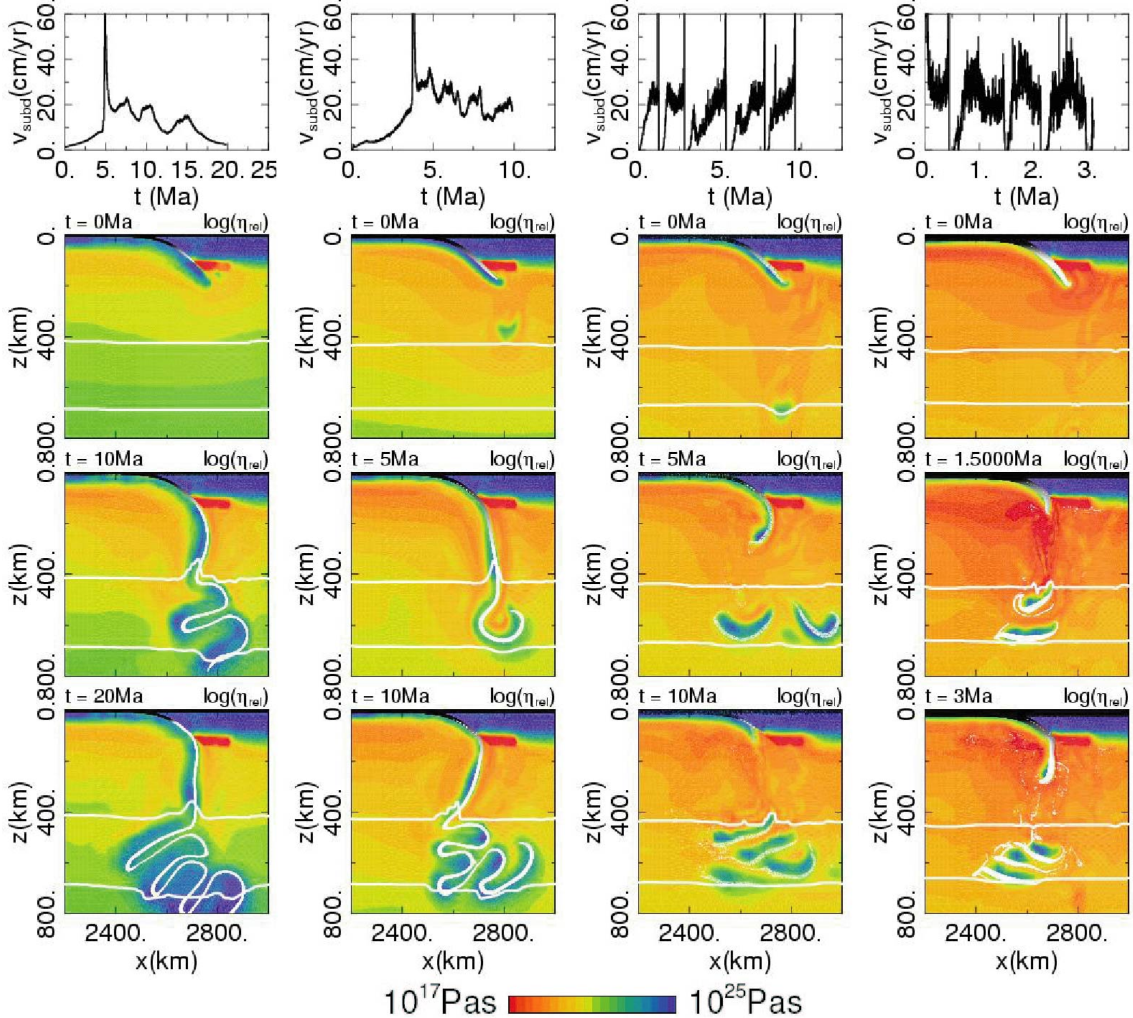

Figure 3: Model results for the lower yield stress case: $\tau_y = 100$ MPa. See Figure 2 for plot description.

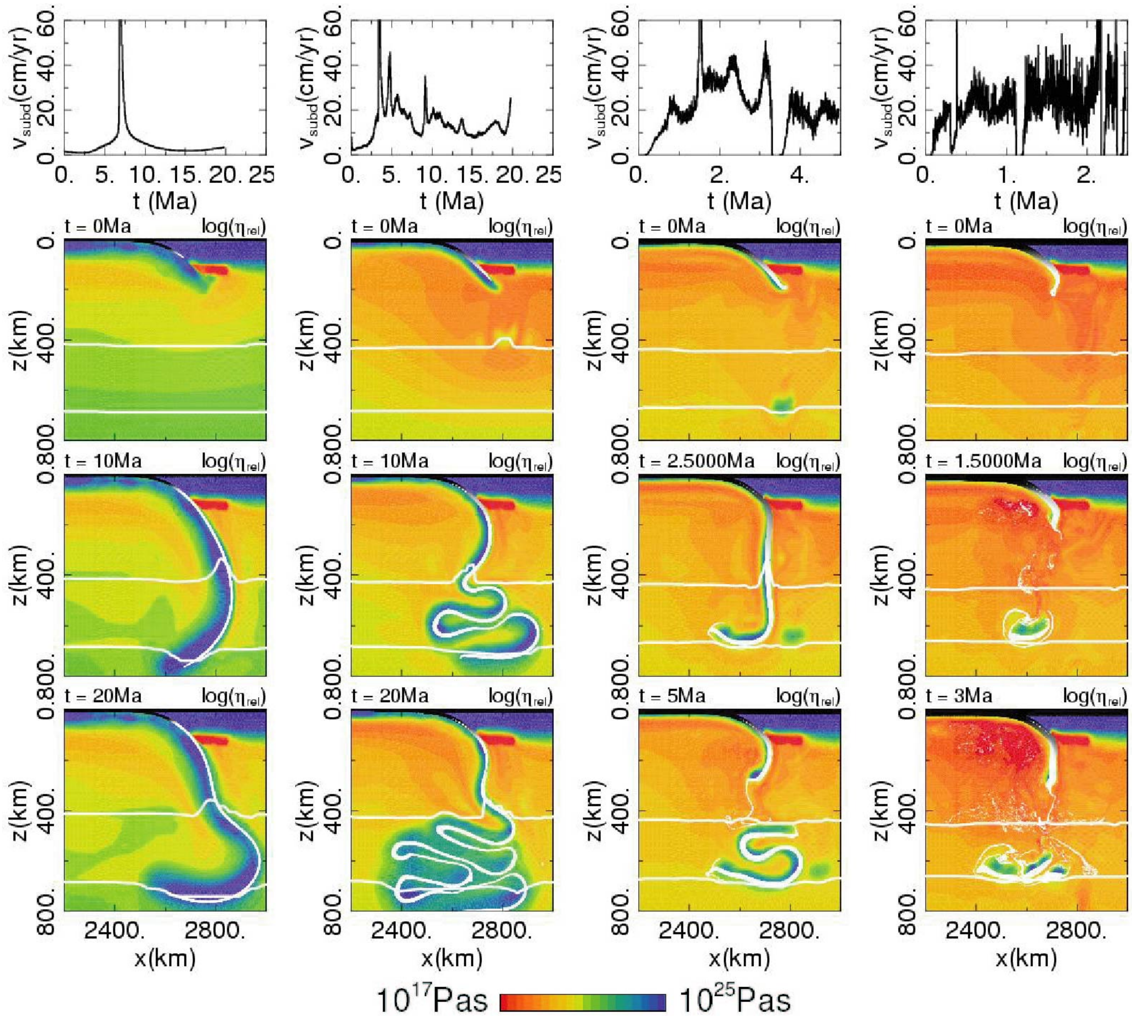

Figure 4: Model results for the higher yield stress case: $\tau_y = 1$ GPa. See Figure 2 for plot description.

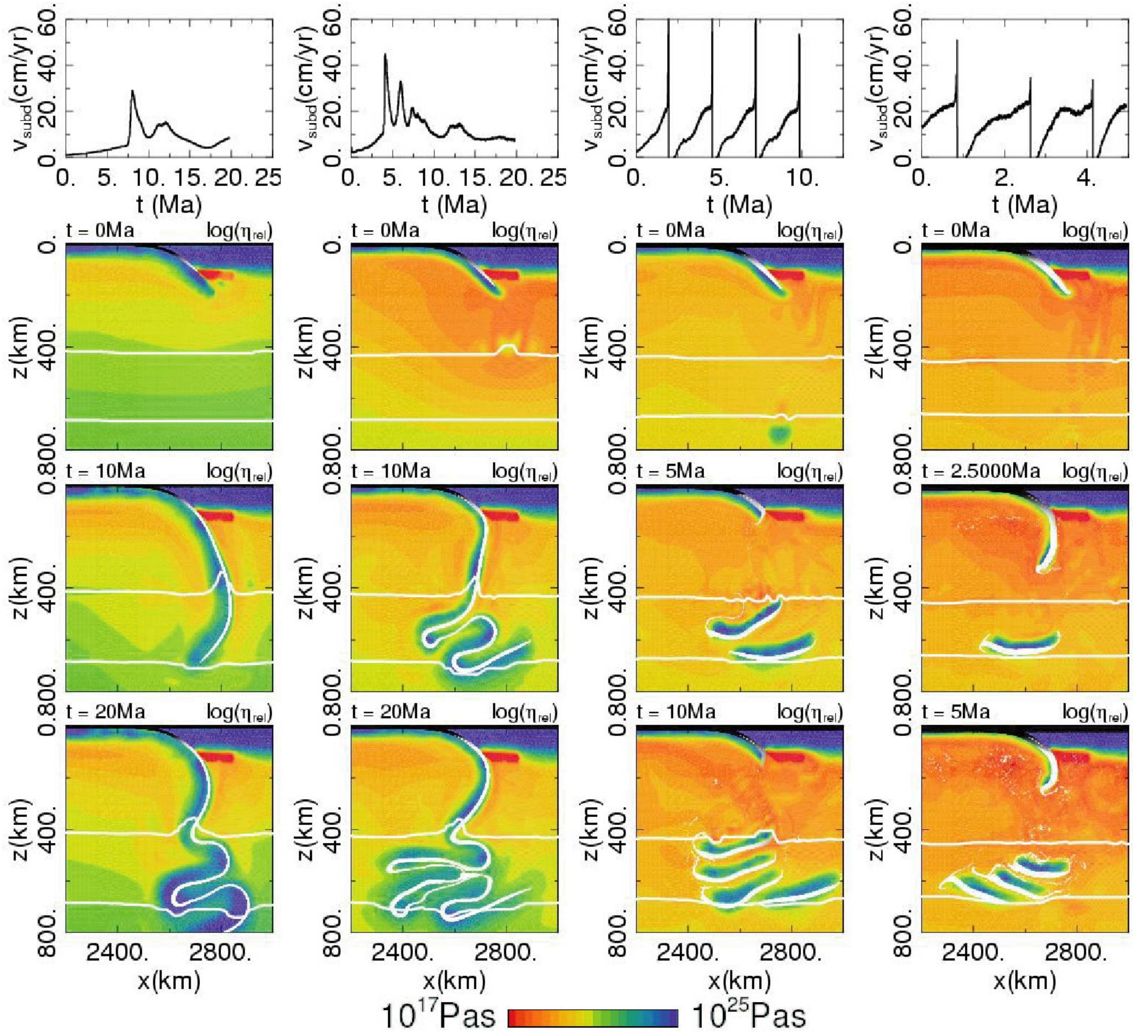

Figure 5: Model results for the calculations with a non-zero fault friction f_f = 5 MPa per c/yr subduction velocity. See Figure 2 for plot description.

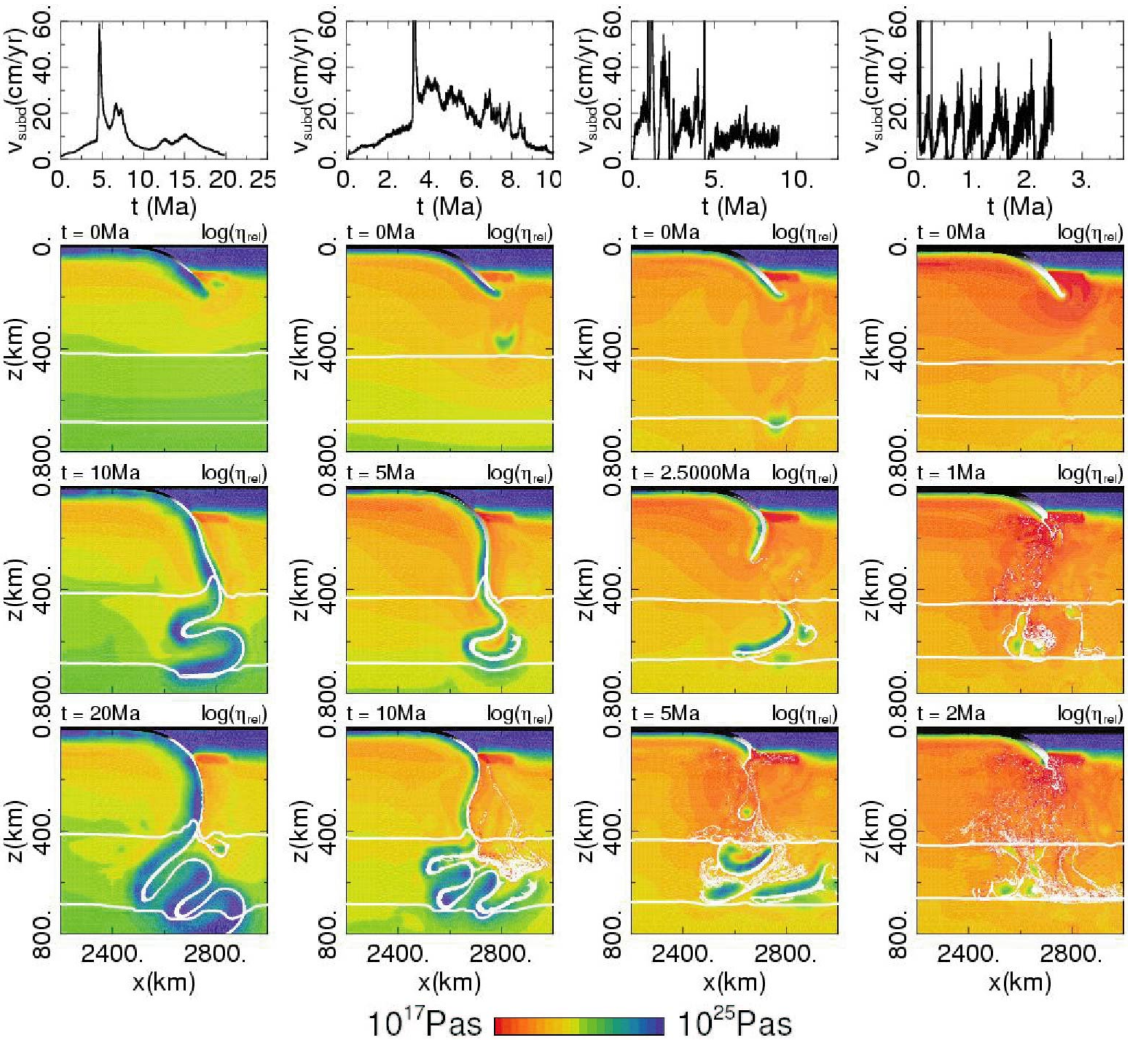

Figure 6: Model results for the calculations in which the deep decoupling is achieved by a weak subducting crust instead of a weak mantle wedge. See Figure 2 for plot description.

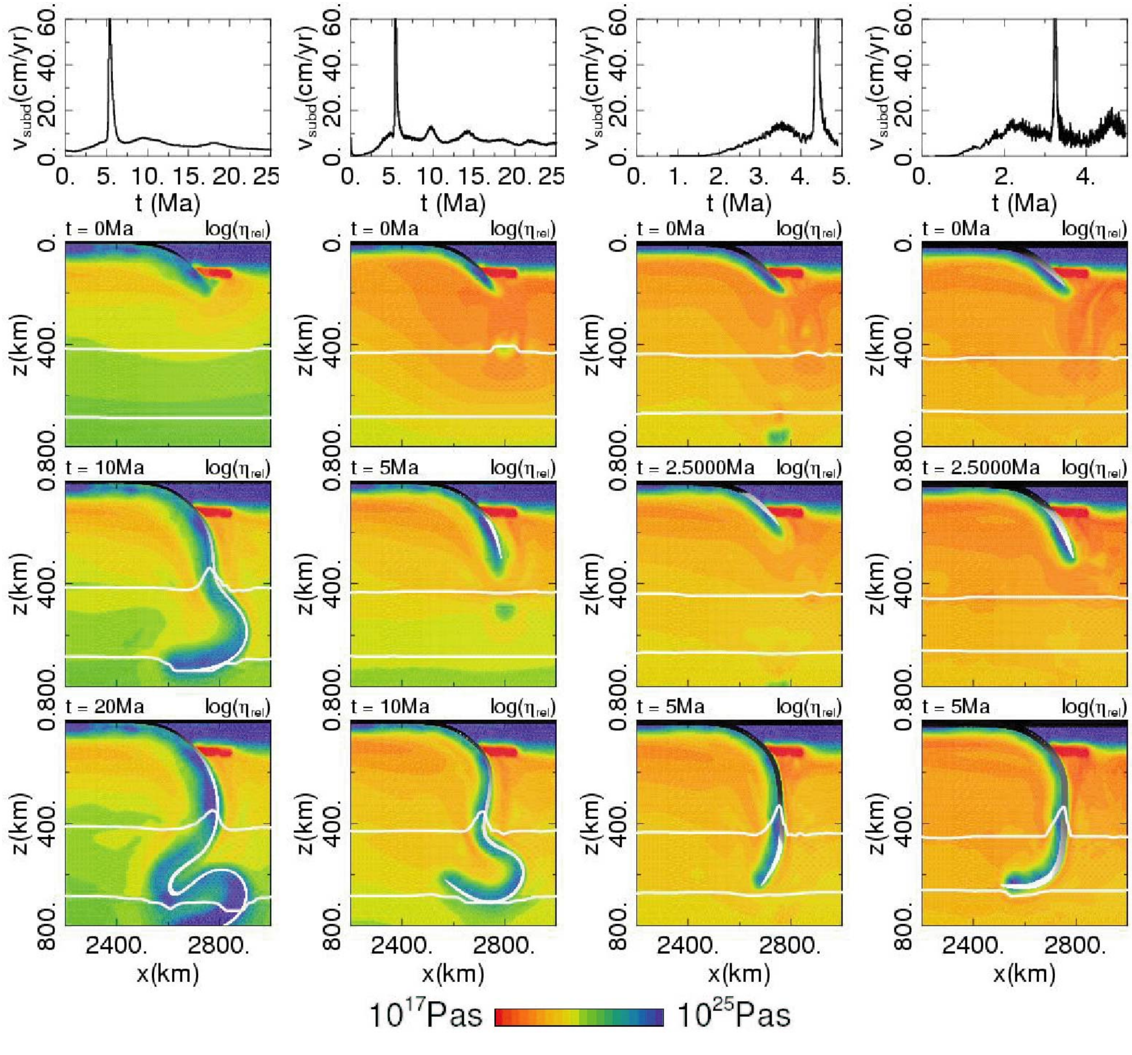

Figure 7: Model results for the calculations with slow eclogitization kinetics: complete transition takes 5 Ma (whereas it is 1 Ma in the default model). See Figure 2 for plot description.

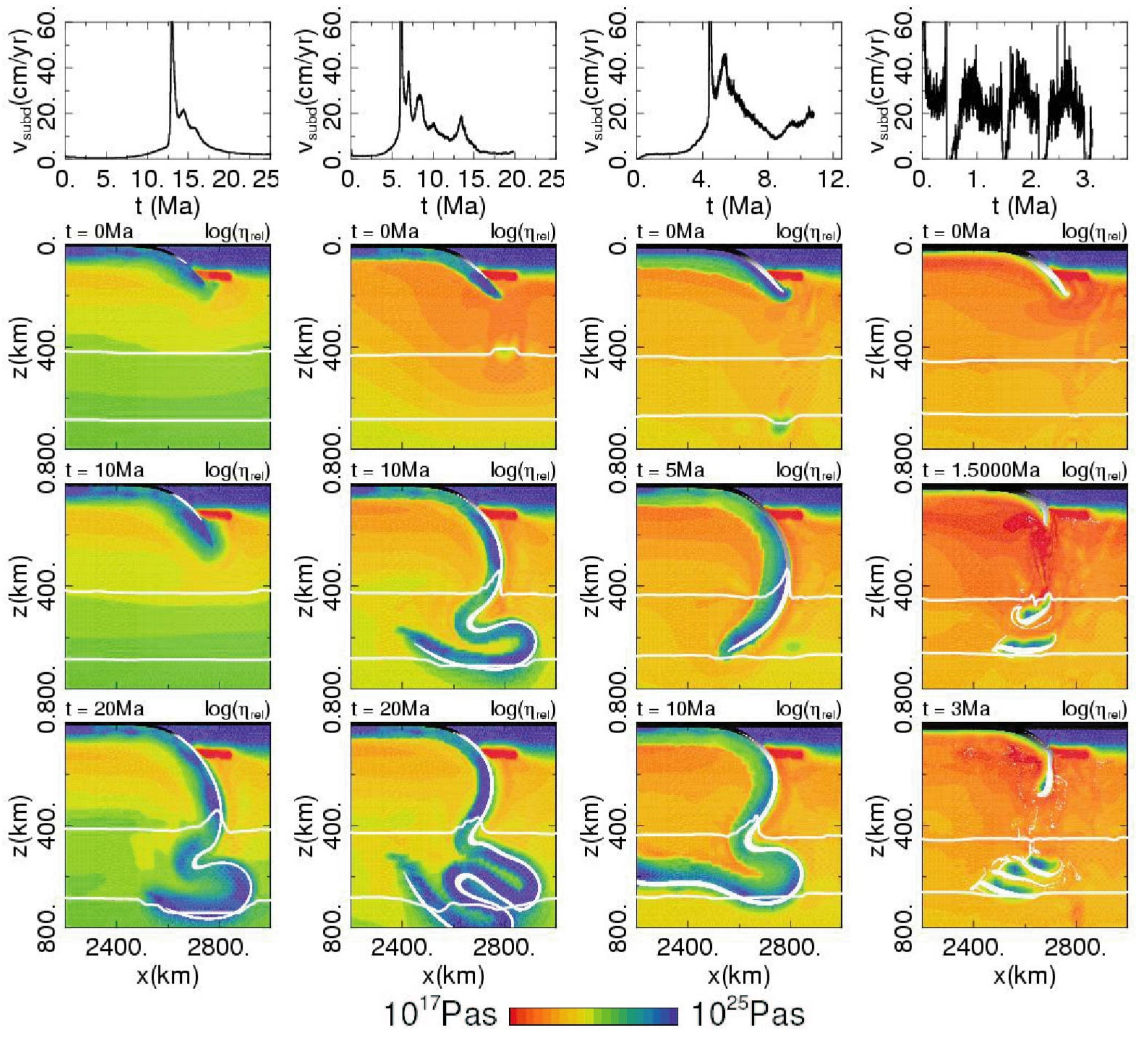

Figure 8: Model results for the calculations with a 100-fold stronger harzburgite layer. See Figure 2 for plot description.

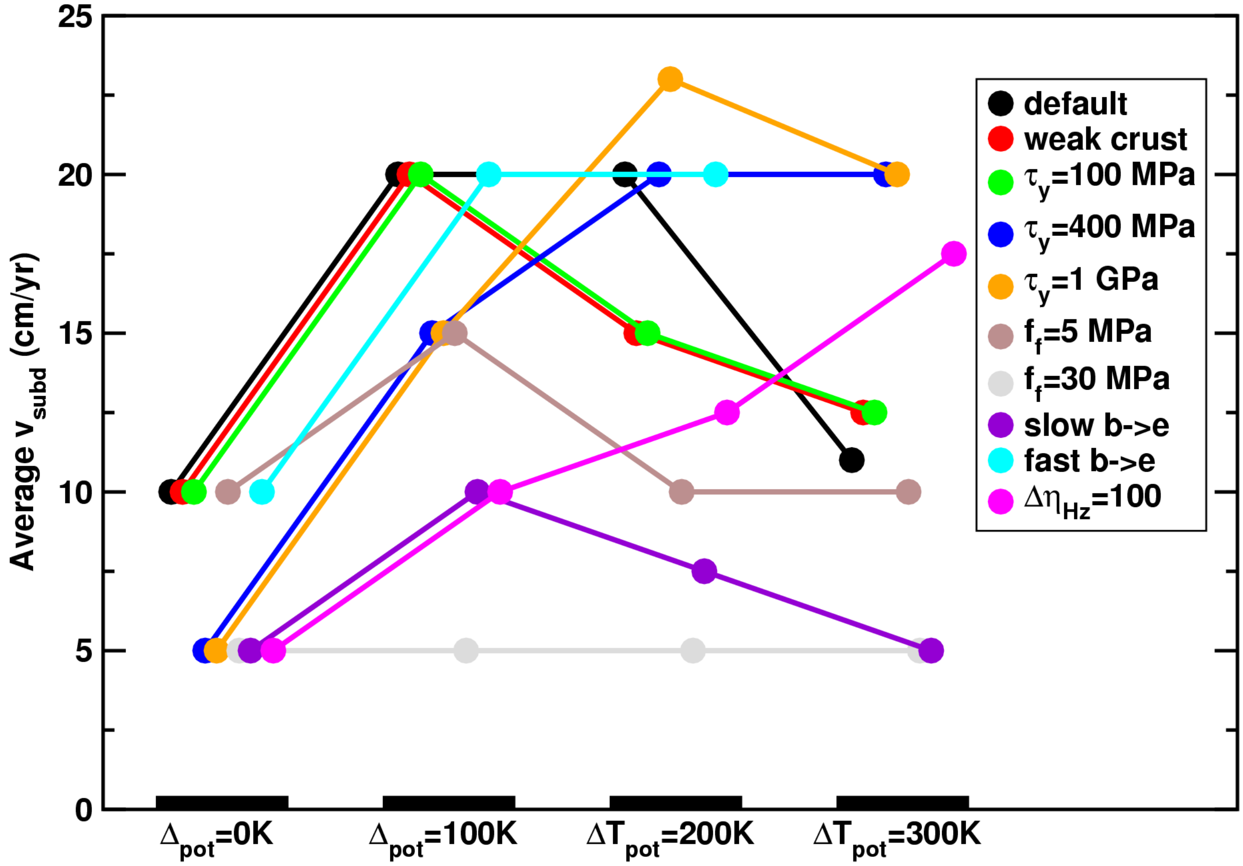

Figure 9: Compilation of the average subduction models in all presented calculations.

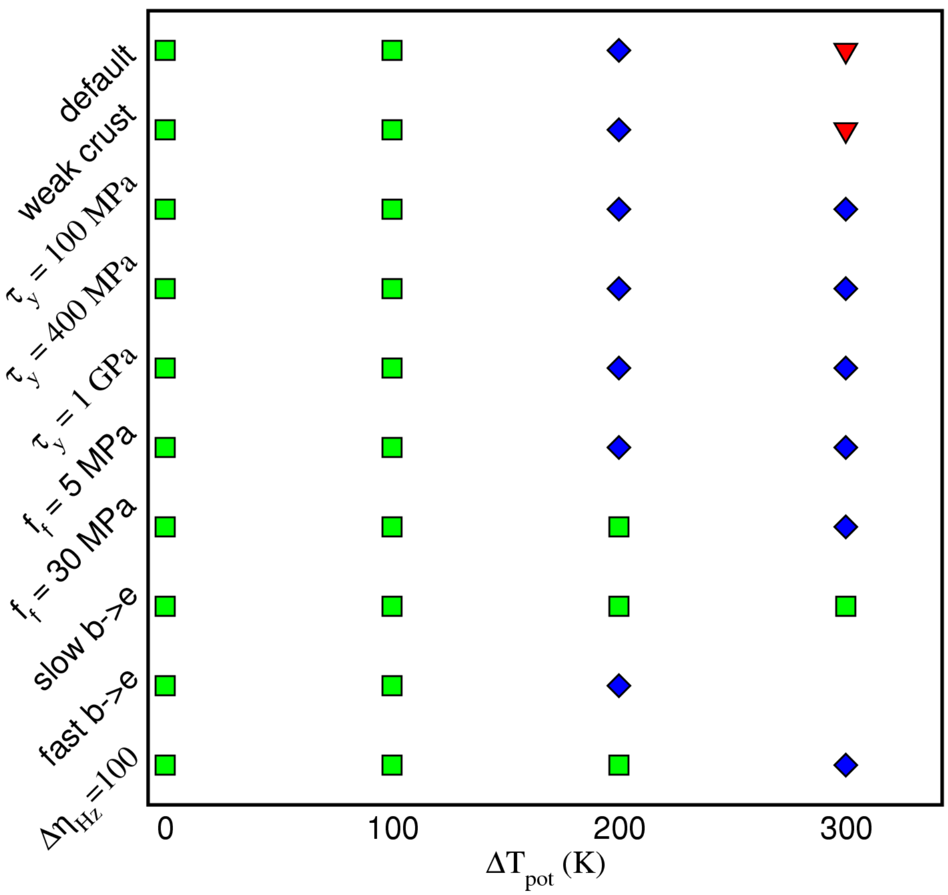

Figure 10: Compilation of the subduction style of all presented calculations. Green blocks indicate a subduction style like at present. Blue diamond indicate frequent slab detachment events, and red triangles denote no continuing subduction.

Symbol	Meaning	Value used	Dimension
A_m	Pre-exponential flow law parameter	–	$\mathrm{Pa}^{-n}\ \mathrm{s}^{-1}$
C	Composition parameter	–	–
c_p	specific heat	1250	$\mathrm{J\ kg^{-1}\ K^{-1}}$
E_m^*	rheological activation energy	–	$\mathrm{J\ mol^{-1}}$
f_f	fault friction	–	MPa
H	radiogenic heat production	–	$\mathrm{W\ m^{-3}}$
k	thermal conductivity	4.13	$\mathrm{W\ m^{-1}\ K^{-1}}$
n_m	viscosity stress exponent	–	–
n_y	yield stress exponent	10	–
Q_L	Latent heat release across a phase transition	–	$\mathrm{J\ kg^{-1}}$
R	gas constant	8.3143	$\mathrm{J\ K^{-1}\ m^{-3}}$
T	temperature	–	°C
T_{pot}	potential temperature	–	°C
t	time	–	s
$\vec{u}$	velocity $\vec{u} = (v, w)^T$	–	$\mathrm{m\ s^{-1}}$
V_m^*	activation volume	–	$\mathrm{m^3\ mol^{-1}}$
v_{subd}	resulting buoyancy-driven subduction velocity	–	$\mathrm{cmyr^{-1}}$
v_{ini}	initially imposed subduction velocity	–	$\mathrm{cmyr^{-1}}$
α	thermal expansion coefficient	3×10^{-5}	$\mathrm{K^{-1}}$
Γ_k	phase functions for all k mantle phase transitions	–	–
γ_k	Clapeyron slope of the k-th phase transition		
	400 km phase transition	3	$\mathrm{MPa\ K^{-1}}$
	670 km phase transition	−2.5	$\mathrm{MPa\ K^{-1}}$
ΔP	non-dimensional hydrodynamic pressure	–	–
ΔT_{pot}	change of T_{pot} with respect to 1350^{o}C	–	°C
$\Delta\rho$	total density variation with respect to ρ_0		$\mathrm{kg\ m^{-3}}$
$\Delta\rho_c$	compositional density relative to mantle material		
	basalt	−500	$\mathrm{kg\ m^{-3}}$
	harzburgite	−75	$\mathrm{kg\ m^{-3}}$
$\delta\rho_k$	density difference across the k-th phase transition		
	400-km phase transition	264	$\mathrm{kg\ m^{-3}}$
	670-km phase transition	330	$\mathrm{kg\ m^{-3}}$
$\dot{\epsilon}_{ij}$	$\dot{\epsilon}_{ij} = \partial_j u_i + \partial_i u_j$ = strainrate tensor	–	$\mathrm{s^{-1}}$
$\dot{\epsilon}$	2$^{\mathrm{nd}}$ invariant of the strainrate	–	$\mathrm{s^{-1}}$
$\dot{\epsilon_y}$	reference strainrate in yield strength determination	1×10^{-15}	$\mathrm{s^{-1}}$
η	viscosity	–	Pa s
ρ_0	mantle density	3300	$\mathrm{kg\ m^{-3}}$
τ_{ij}	deviatoric stress tensor	–	Pa
τ	2^{nd} invariant of the stress tensor τ_{ij}	–	Pa
τ_y	yield stress for strainrate $\dot{\epsilon}_y$	–	Pa

Table 1: Notations

mtrl.	mech.	A (Pa$^{-\mathrm{n}}$/s)	n	E^* (J/mol)	V^* (cm^3/mol)
crust	disl.	8.8×10^{-25}	3.4	260×10^3	10
mantle	diff.	1.92×10^{-11}	1.0	300×10^3	4.5
mantle	disl.	2.42×10^{-16}	3.5	540×10^3	14

Table 2: Rheology parameters for the deformation mechanisms of crust and mantle material. Crustal diffusion creep is not included.